

Studying the FRP-Concrete Bond Behavior of Normal and Light-Weight Concrete Using FEM

Ali Oday Hilal

Ahid Zuhair Hamoody

Ahmed Sagban Saadoon

Department of Civil Engineering, College of Engineering, University of Basrah, Basrah, Iraq.

ali.adi61@yahoo.com

msc_eng_ah@yahoo.com

ahmsag@gmail.com

Submission date:-	Acceptance date:-	Publication date:-
--------------------------	--------------------------	---------------------------

Abstract

The main objective of the present study is to investigate the behavior of FRP-concrete bond of two types of concrete (normal and light weight concrete) using different concrete properties. For this purpose, a model of single shear test was selected and modeled using ANSYS program to study the FRP-concrete bond. The modeling was represented in two ways: with epoxy material (epoxy model) and without epoxy material (full bond model). These two models were formulated and used in the analysis process. Different models of two types of concrete (normal and light weight concrete) were analyzed in order to study bond behavior. In general, the full bond model gave results of more good agreement with the available experimental results than the epoxy model. The average difference between the experimental and analytical failure load was 5.35% and 10.32% for the full bond and epoxy model, respectively. It was found that the increasing in compressive strength of concrete leads to increasing in the bond capacity and the greater concrete compressive strength the better utility of the CFRP sheet. As the compressive strength was increased from 20 to 40MPa, the bond strength of normal concrete and light weight concrete models increased by about 81% and 106%, respectively.

Keywords: FRP, Bond, Bond capacity, Single Shear Test.

1. Introduction

FRP (fiber reinforced polymers) are composite comprise fibers of high tensile strength within a polymer matrix. The FRP material is generally consisting of carbon, aramid, or glass fibers in a polymeric matrix (e.g., thermosetting resin) [1]. Over the last decennium there has been important growth in the use of FRP composite materials as construction materials in structural engineering. The light weight of these materials and their formability of FRP reinforcement make them easier to install. These materials are noncorrosive, nonmagnetic, and generally resistant to chemicals so they are an excellent option for many applications as external reinforcement and repairing structures (columns, beams, slabs, walls, chimney and tunnels). The use of external FRP reinforcement may be generally classified as flexural strengthening, improving the

confinement and ductility of compression members, and shear strengthening [2]. There are three common types of FRP materials; carbon, glass and aramid fibers. The carbon fiber reinforced polymer (CFRP) is the most type that used for strengthening and repairing structural elements [3].

The most important issue in the field of strengthening reinforced structures with FRP plates or sheets is the proper design against debonding failure (loss of composite action between concrete and FRP). There are various debonding failure modes such as cover separation, plate and interfacial debonding, intermediate flexural crack induced interfacial debonding, and critical diagonal crack induced interfacial debonding [4]. Therefore, the behavior of the interface between FRP and concrete support is one of the main elements controlling debonding failures in RC structures strengthened with FRP sheets or plates, Fig. 1 shows some typical debonding failures.

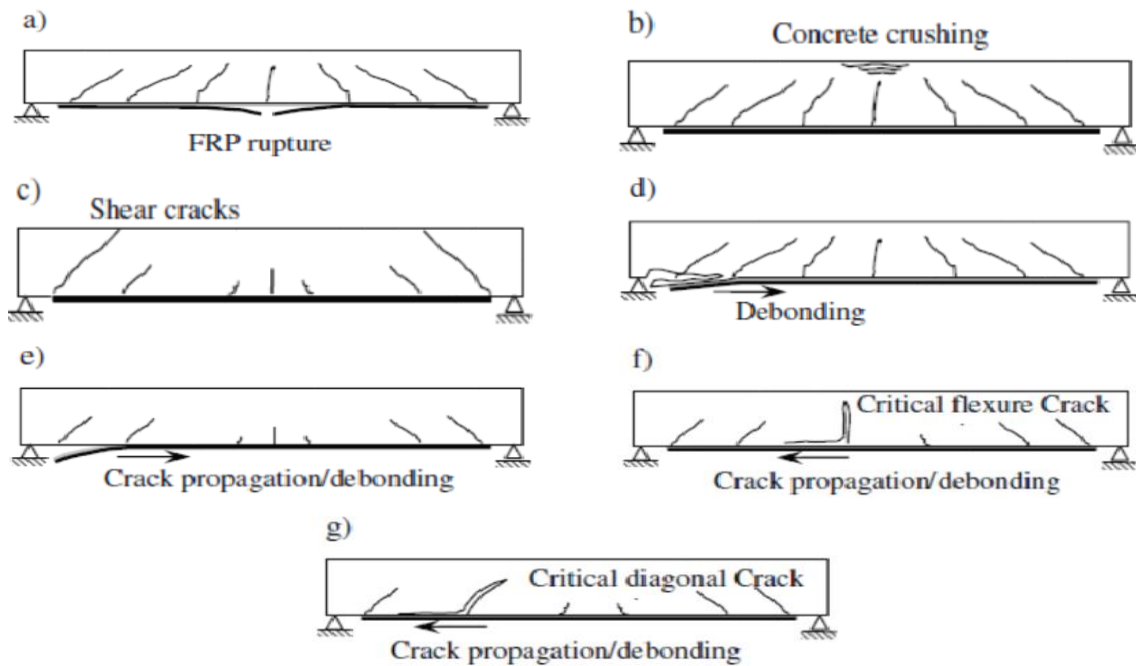


Figure 1. Failure modes of RC beams strengthened with FRP strips [4]

2. Bond Strength Test

Many models have been suggested for the bond strength between concrete and FRP laminates. Some models were based on empirical equations calibrated with experimental results, and others were based on fracture mechanics theories and they contain many variables calibrated with

experimental results, the design models were also suggested by assuming simple assumptions and verifying them against test results [5] –[15]. In all models, the stress state is simulated by a “shear test” or “pull-off test” on a concrete specimen with bonded FRP strip, as shown in Fig. 2, in which one or two FRP strips externally bonded to one or two opposite sides of a concrete prism (block) by an adhesive resin (epoxy), then a tensile force is applied to the FRP strip from one side of the concrete prism (single shear test) or from two opposite side of the concrete prism (double shear test) using hydraulic machine.

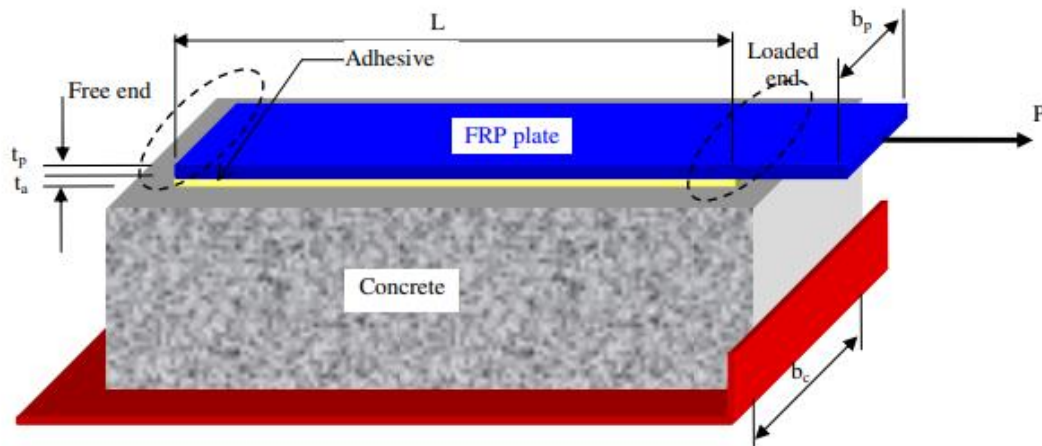


Figure 2. Single shear test specimen [5]

3. Finite Elements Modeling

In order to study the behavior of FRP-concrete bond, a model of single shear test (a concrete prism bonded from one side with CFRP sheet) is selected and modeled using ANSYS program. A direct tensile force is applied to the CFRP sheet increasingly up to failure. This model was adopted by many codes and researchers to calculate or study the strength, stress and effective length of the bond between the concrete and CFRP sheets or strips [16], [17], [18]. The modeling was represented in two ways: with epoxy material (epoxy model) and without epoxy material (full bond model).

3.1. Material Modeling

The concrete is a brittle material and had different behavior in compression and tension. A typical stress-strain curve for normal weight concrete is shown in Fig. 3. The stress-strain curve for concrete in compression is linearly elastic up to approximate 30 percent of the maximum compressive strength. Above this point, the stress increases gradually up to the peak compressive strength σ_{cu} after this point, the curve descends into a softening region, and finally crushing

failure occurs at an ultimate strain ϵ_{cu} . According to ACI-318-14 Code [19], ultimate compressive strength occurs at a strain (ϵ_o) of approximately (0.002). Also, the code specifies that the ultimate strain (ϵ_u) be taken as (0.003). In tension, the stress-strain curve for concrete is similar to the behavior observed in uniaxial compression and approximately linearly elastic up to the maximum tensile strength. After this point, the crack occurs in concrete and the strength decreases gradually to zero [20]. The tensile strength of concrete is typically about 10 to 15 percent of compressive strength of concrete [19]. Poisson's ratio (ν) of concrete has been observed to remain approximately constant and ranges from about 0.15 to 0.22 up to a stress level of 80% f'_c . Beyond this level, Poisson's ratio increases rapidly and values in excess of 1.0 have been measured. In this study, a value of 0.2 is used for all types of concrete.

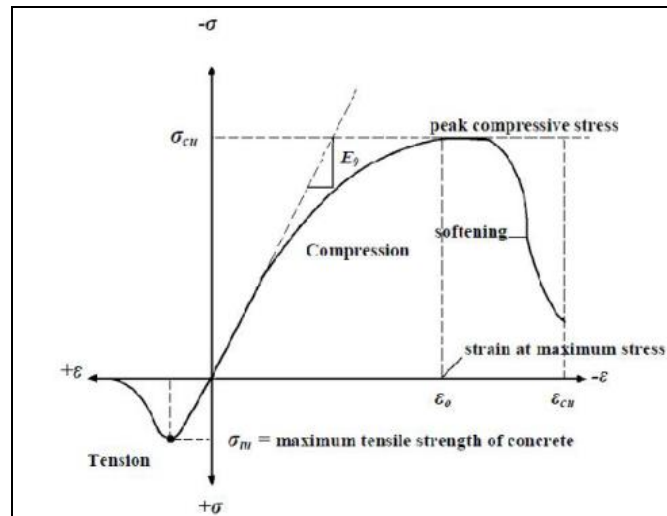


Figure 3. Typical uniaxial compressive and tensile stress-strain curve for concrete [21]

For normal weight concrete, the Desayi and Krishnan model [22] is adopted in this study to simulate the multi-linear isotropic stress-strain curve. The modulus of elasticity (E_c) is generally taken as a function of compressive strength of concrete (f'_c). The modulus of elasticity for concrete can be calculated with accepted accuracy from the empirical equation recommended by ACI 318-14 as,

$$E_c = 4700 \times \sqrt{f'_c} \quad (\text{MPa}), \quad (1)$$

where f'_c is the ultimate compressive strength in (MPa).

For the case of light weight concrete, the same equations of normal weight concrete are used with a modification factor (λ). This modification factor is multiplied by the modulus of elasticity of normal concrete (Eq. 1) to get the modulus of elasticity of light weight concrete, as

$$E_c = 4700 \times \lambda \times \sqrt{f'_c}, \quad (2)$$

where λ is a modification factor reflecting the reduced mechanical properties of light weight concrete relative to normal weight concrete of the same compressive strength ($\lambda = 0.85$ for sand-light weight aggregate concrete) [9].

FRP materials consist of two constituents. First constituent is the reinforcement, which is embedded in the second constituent, a continuous polymer called the matrix [23]. The FRP composites are considered as orthotropic elastic materials in the model of finite element; so their properties are different in both directions. In the present study, Young's modulus in the lateral direction and shear modulus is assumed to be zero due to the unidirectional property of the FRP material and contributions in lateral and shear stiffness of the FRP sheet can be assumed to be negligible, since sheet is at most loaded in the longitudinal direction [24]. The value of 0.3 has been taken for Poisson's ratio, and linearly elastic stress-strain relationship behavior, Fig. 4, is considered for CFRP sheets which do not exhibit any plastic behavior before rupture.

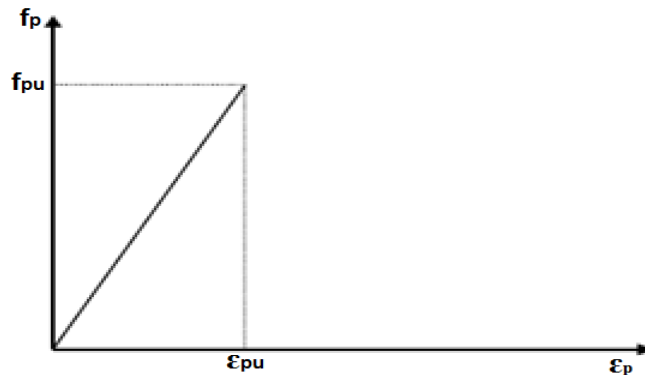


Figure 4. Idealized stress-strain relationship for CFRP strips [25]

3.2. Materials Details

A concrete prism with dimensions of (350×150×150mm) bonded with an CFRP sheet of (95mm) length and (25mm) width is selected in the present study to represent the single shear test. These dimensions and measurements have been used in experimental tests by other researchers [16]. Fig. 5 shows a typical finite element model in ANSYS program that used in this study. The SOLID65 and SHELL41 elements are used to model the concrete and CFRP sheets, respectively.

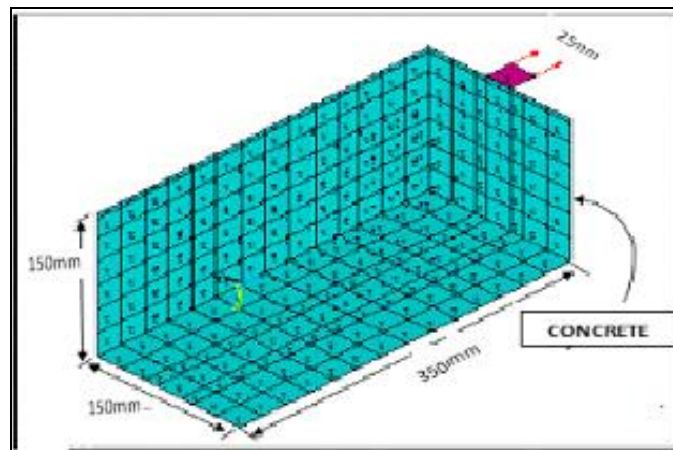
The 8-node SOLID65 brick element is a 3-D element used for solids modeling. This element is capable of cracking in tension, crushing in compression and modeling nonlinear material properties, while SHELL41 is a 3-D element having membrane (in-plane) stiffness but no bending (out-of-plane) stiffness. It is intended for shell structures where bending of the elements is of secondary importance [26]. In this study, the SHELL41 element is assumed to have a constant thickness of (1.65mm). In the case of representing a model with epoxy material between the concrete and CFRP sheet, the SOLID65 element is also used to model the epoxy material, as a contact element, and the linearly elastic stress-strain relationship behavior is considered for the epoxy material. The epoxy with nominal thickness of (1mm) is considered along the CFRP sheet to achieve full integrity between the two materials. Tables 1 and 2 show the chosen elements type and materials properties of the CFRP sheets and epoxy that used in the present study.

Table 1. Elements' type

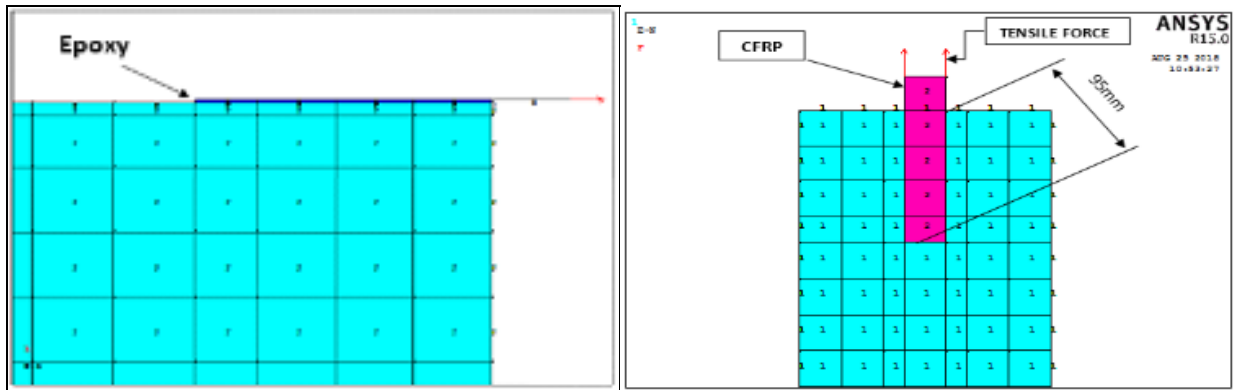
Material	Element type
Concrete	SOLID65
CFRP	SHELL41
Epoxy	SOLID65

Table 2. FRP and epoxy properties

Material	Modulus of elasticity (GPa)	Tensile strength (MPa)	Poison's ratio
CFRP	256	4114	0.3
Epoxy	36.1	39.4	0.3



(a) Isometric view



(b) Side view

(c) Top view

Figure 5. Typical finite element model

3.3. Meshing of Models

To get good results from the SOLID65 and SHELL41 elements, the use of a rectangular mesh is recommended [26]. Therefore, the mesh was set up such that square or rectangular elements were created. A convergence study was performed to choose the best mesh size. Firstly, a coarse meshing was used, and then it was minified gradually until the least error was achieved by comparing the obtained results with the available experimental results. At the end, it was found that the element size of (25×25×25mm), which yields more than 500 elements, gave the most accurate results compared with the experimental results.

3.4. Verification of Formulated Models

To verify the validity and accuracy of the present formulated finite element models (epoxy model and full bond model), the obtained analytical results from these models are compared with the experimental results of specimens tested by Jain [17] and Zhao [18]. The results of this comparison are showed in Fig. 6. The average difference between the experimental and analytical failure load was 5.35% and 10.32% for the full bond and epoxy model, respectively. The analytical results of both models show good agreement with the experimental values. In general, the full bond model gives results of more good agreement with the experimental results than the epoxy model, so the full bond model will be used to study the effect of some concrete properties on the concrete-FRP bond.

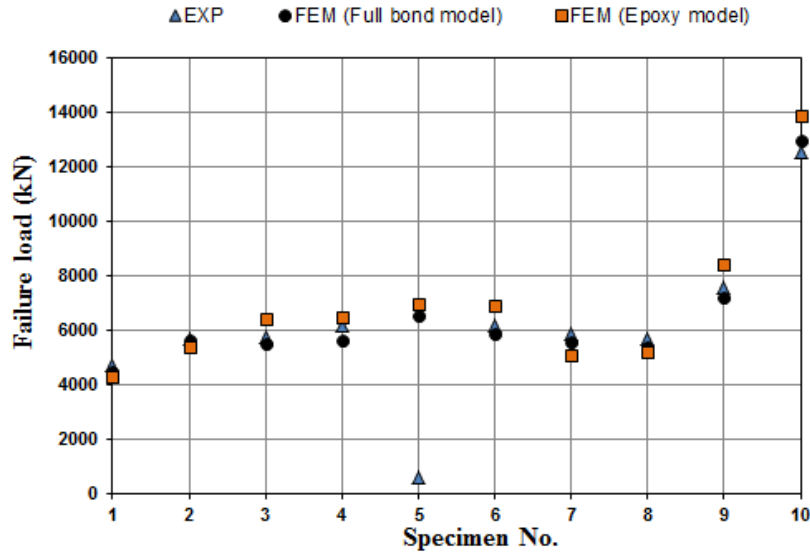


Figure 6. Comparison between available experimental results and present analytical results

4. Results and Discussion

4.1. Analysis of Normal Weight Concrete Models

In order to investigate the effect of variation of concrete compressive strength on the bond between the concrete and CFRP sheet and hence to understand how and how much this bond would be changed accordingly, different compressive strengths ranged between 20 and 40MPa are used (since it is the usual and most widely used range of normal concrete strength). Five specimens with different f'_c , ranged from 20 to 40MPa with an increment of 5MPa, are modeled and analyzed using the formulated full bond model for each specimen. Each analysis process included investigating the bond capacity and stress distribution. Fig. 7 shows the bond capacity (ultimate failure load) for different compressive strengths.

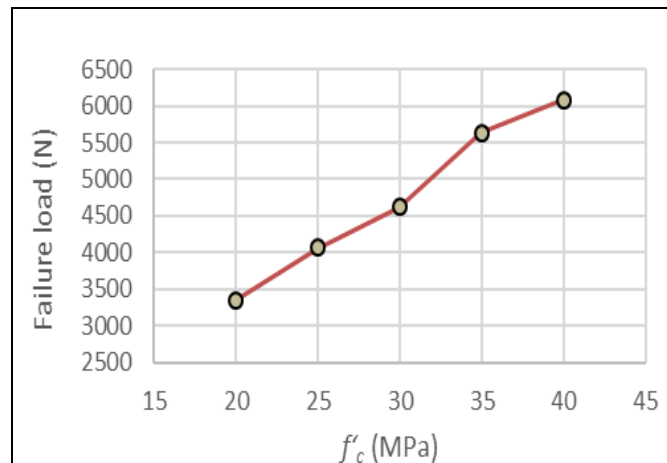
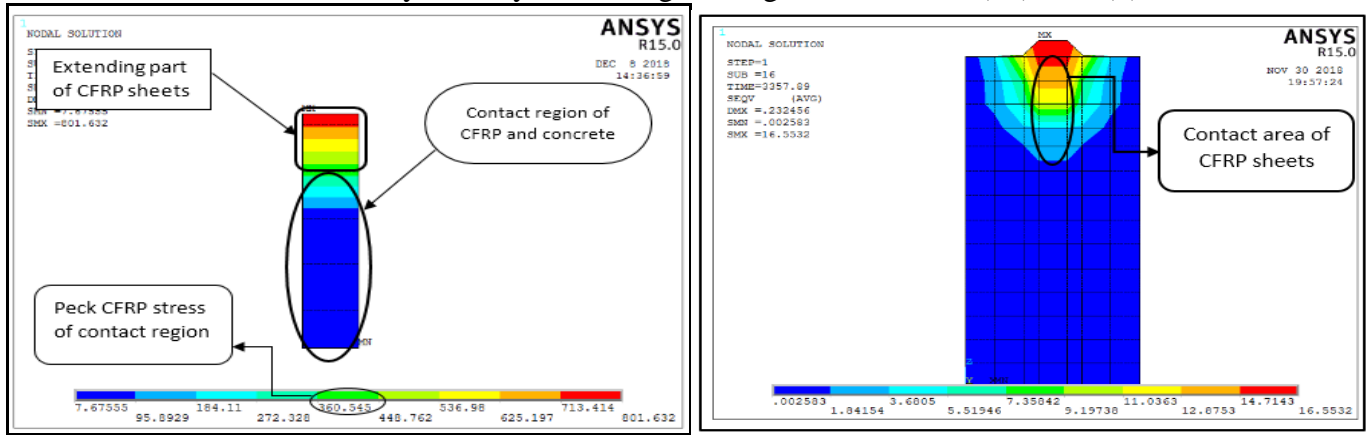


Figure 7. Bond capacity of normal concrete versus concrete compressive strength

As can be noticed from this figure, the relationship between bond capacity and compressive strength of concrete is approximately a linear relationship. The bond strength increases by about 38% as the compressive strength increases from 20 to 30MPa, while it increases by about 31.5% as the compressive strength increases from 30 to 40MPa. In average, it increases by about 81% as the compressive strength increases from 20 to 40MPa. From these results, it is obvious that the increasing in compressive strength of concrete leads to increasing in the bond capacity. However, the increasing ratio in bond capacity decreases as the compressive strength increases.

The stress value and its distribution are very important in this study to determine the case of failure of each model and to understand the condition of stress transferring from one material to another. Figs. 8-10 show the stress distribution in CFRP sheet and concrete. Within the contact region between the concrete and CFRP sheet, the maximum stress of CFRP sheet is equal to 390, 503, 622, 673, and 715MPa for models with compressive strength of 20, 25, 30, 35, and 40MPa, respectively. As the concrete compressive strength increases, the maximum stress of CFRP sheet increases in approximately a linear relationship. The CFRP sheet undergoes greater stresses as the concrete compressive strength increases. So it can be said that, the greater concrete compressive strength the better utility of the CFRP sheet. For all models, the maximum stress of CFRP sheet is less than the ultimate strength of CFRP sheet, which equals 4114MPa. The CFRP maximum stress occurs at points, within the contact region, nearest to the loaded end, then the stress decreases gradually in a fast manner as moving away from the loading side through approximately one quarter of the contact region length then it decreases slowly along the rest length of the contact region.

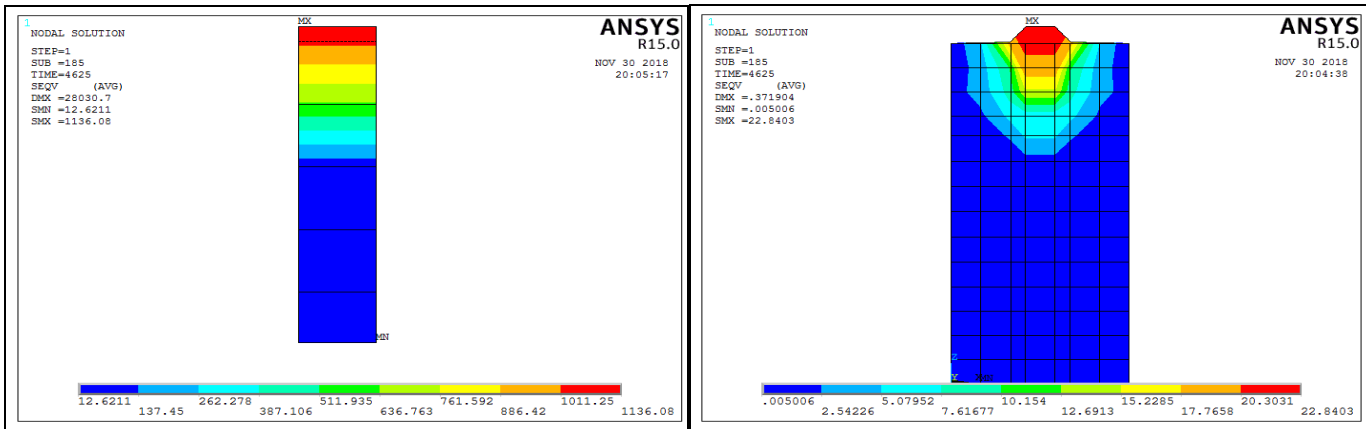
For concrete, the maximum stress is equal to 16.5, 20.5, 22.8, 29.8, and 31.5MPa for models with compressive strength of 20, 25, 30, 35, and 40MPa, respectively. For all models, this maximum stress of concrete occurs at points contacted to CFRP sheet and nearest to the applied tensile load, then the stress in concrete decreases gradually along the contact area with the CFRP sheet. In general, the concrete stress at all points along and adjacent to the contact area, except the farthest small part from the loading side, exceeds both the ultimate tensile strength and the ultimate shear strength of concrete that specified by the ACI code [19] as $(0.1 f'c)$ and $(0.167 \sqrt{f'c})$, respectively.



(a) Stress distribution in CFRP sheet

(b) Stress distribution in concrete

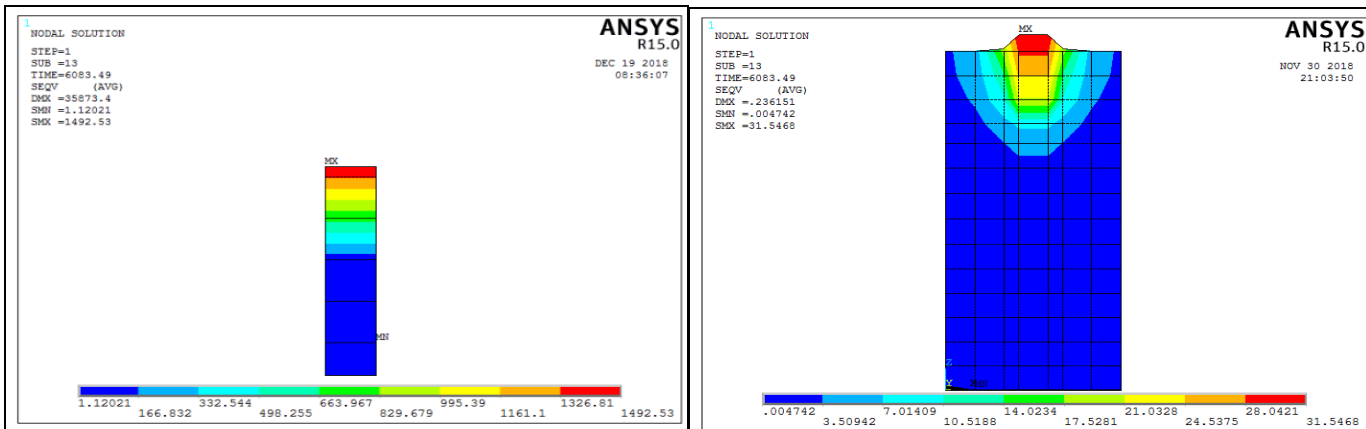
Figure 8. Stress distribution of normal concrete model with $f'c = 20\text{MPa}$



(a) Stress distribution in CFRP sheet

(b) Stress distribution in concrete

Figure 9. Stress distribution of normal concrete model with $f'c = 30\text{MPa}$



(a) Stress distribution in CFRP sheet

(b) Stress distribution in concrete

Figure 10. Stress distribution of normal concrete model with $f'c = 40\text{MPa}$

4.2. Analysis of Sand-Light Weight Aggregate Concrete Models

For light weight concrete, the ACI [19] stated that the modulus of elasticity of concrete is given above. In order to investigate the effect of using light weight concrete with various concrete compressive strength on the bond between the concrete and FRP sheet and hence to understand how and how much this bond would be changed accordingly. Different concrete compressive strengths ranged between 20MPa and 40MPa are used. Five specimens with different $f'c$, ranged from 20 to 40MPa with an increment of 5MPa, are modeled and analyzed using the formulated full bond model for each specimen. As before, each model will use to investigate the bond capacity and stress distribution. Fig. 11 shows the bond capacity (ultimate failure load) for different compressive strengths. For comparison purpose, the bond capacity for normal concrete, estimated by the same full bond model, is also stated in this figure.

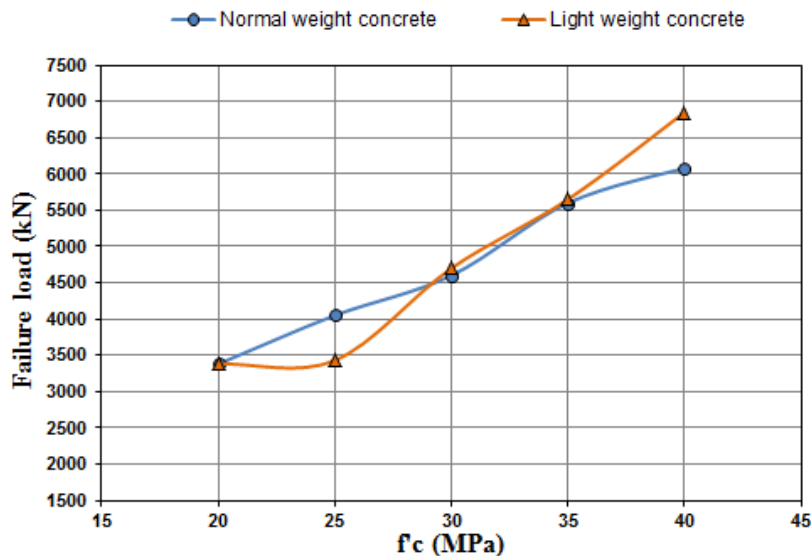
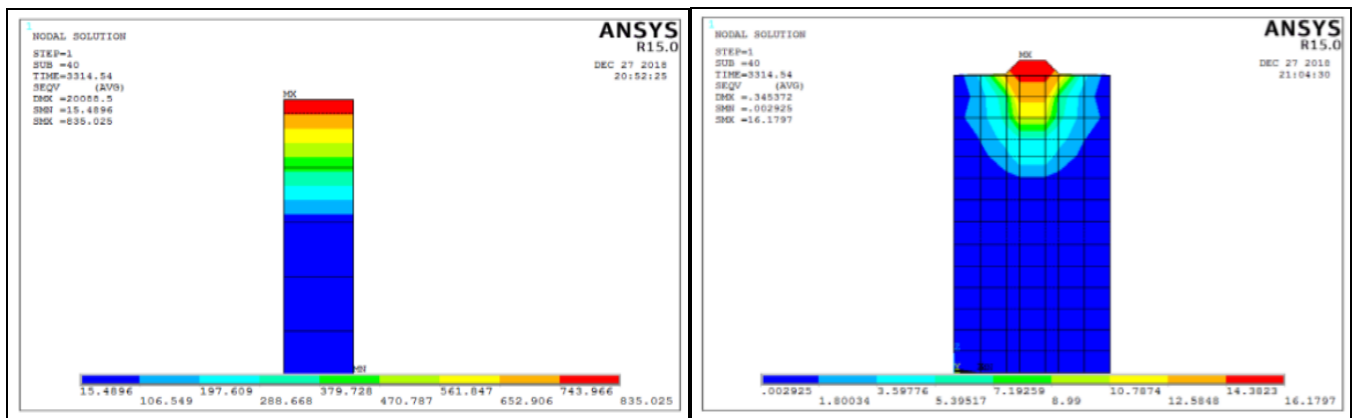


Figure 11. Bond capacity of normal and light weight concrete versus concrete compressive strength

From Fig. 11, the relationship between bond capacity and compressive strength of light weight concrete is approximately linear, as for normal concrete but with a slightly greater slope. The bond strength increases by about 43% as the compressive strength increases from 20 to 30MPa, while it increases by about 44% as the compressive strength increases from 30 to 40MPa. In average, it increases by about 106% as the compressive strength increases from 20 to 40MPa. From these results, it is obvious that the increasing in compressive strength of concrete leads to increasing in the bond capacity. The bond capacity of light weight concrete model is less than that of the corresponding normal concrete for models with $f'c = 20$ and 25MPa, while it is greater than that of the corresponding normal concrete for models with $f'c = 30, 35$ and 40MPa. Therefore, it can be said that the decreasing in concrete modulus of elasticity leads to decreasing in the bond capacity if $f'c < 30$ MPa and increasing in the bond capacity if $f'c \geq 30$ MPa.

The stress distribution in CFRP sheet and concrete are shown in Figs. 12-14. Within the contact region between the concrete and CFRP sheet, the maximum stress of CFRP sheet is equal to 402, 409, 645, 693 and 848MPa for models with compressive strength of 20, 25, 30, 35, and 40MPa, respectively. As the concrete compressive strength increases, the maximum stress in CFRP sheet increases nonlinearly. The CFRP sheet undergoes greater stresses as the concrete compressive strength increases. For all models, the maximum stress of CFRP sheet is less than the ultimate strength of CFRP sheet. As in the case of normal weight concrete of full bond models, the CFRP maximum stress occurs at points, within the contact region, nearest to the loaded end, then the stress decreases gradually in a fast manner as moving away from the loading side through approximately one quarter of the contact region then it decreases slowly along the rest length of the contact region.

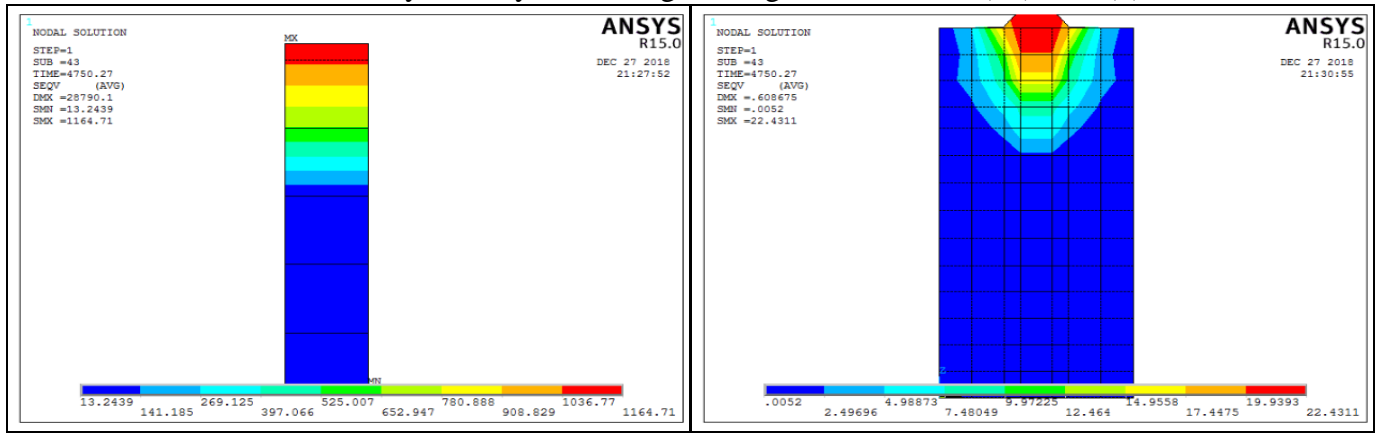
For concrete, the maximum stress is equal to 14, 17.5, 22.4, 29.1 and 33.5MPa for models with compressive strength of 20, 25, 30, 35, and 40MPa, respectively. For all models, the maximum stress of concrete occurs at points contacted to CFRP sheet and nearest to the applied tensile load, then the stress in concrete decreases gradually along the contact area with the CFRP sheet, as in the case of normal concrete. In general, the concrete stress at all points along and adjacent to the contact area (except the farthest small part from the loading side) exceeds both the ultimate tensile strength and the ultimate shear strength of concrete.



(a) Stress distribution in CFRP sheet

(b) Stress distribution in concrete

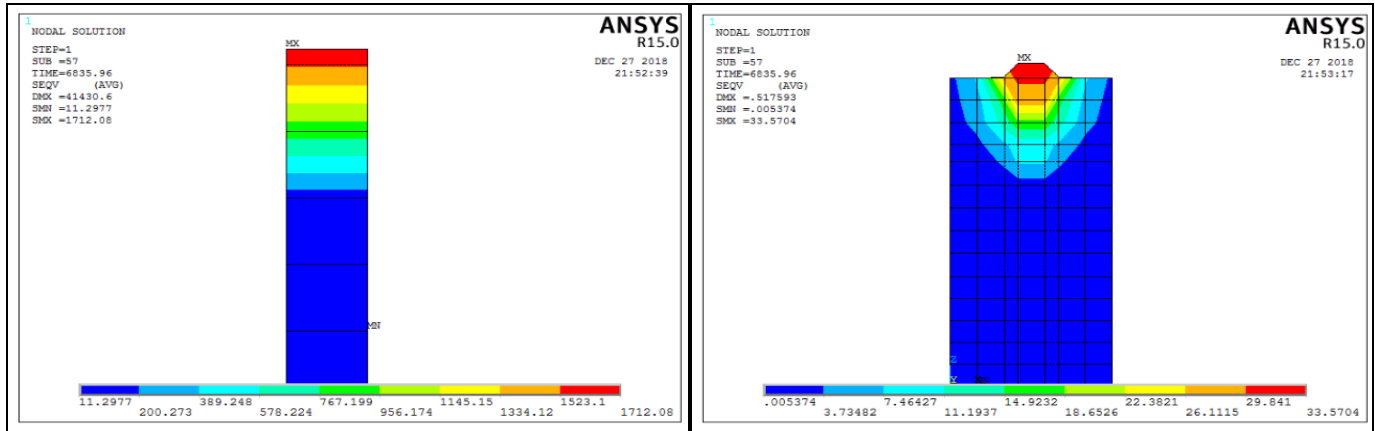
Figure 12. Stress distribution of normal concrete model with $f'c = 20\text{MPa}$



(a) Stress distribution in CFRP sheet

(b) Stress distribution in concrete

Figure 13. Stress distribution of normal concrete model with $f'c = 30\text{MPa}$



(a) Stress distribution in CFRP sheet

(b) Stress distribution in concrete

Figure 14. Stress distribution of normal concrete model with $f'c = 40\text{MPa}$

5. Conclusions

The most important conclusions that can be drawn from the present study are the followings:

- The average difference between the experimental and analytical failure load is 5.35% and 10.32% for the full bond and epoxy model, respectively. Thus, the full bond model gives results of more good agreement with the experimental results than the epoxy model.
- For models with normal concrete, the bond capacity increases by about 81% as the compressive strength increases from 20 to 40 MPa.
- For models with light weight concrete, the bond capacity increases by about 106% as the compressive strength increases from 20 to 40 MPa.
- The relationship between bond capacity and compressive strength of concrete is approximately a linear relationship.

- The FRP sheet undergoes greater stresses as the concrete compressive strength increases. Thus, the greater concrete compressive strength the better utility of the FRP sheet.
- All studied models are failed in the same way by debonding the CFRP sheet due to concrete failure. Therefore, changing the compressive strength and modulus of elasticity of concrete has no effect or does not change the failure mode.
- The bond capacity of light weight concrete models (i.e. decreasing in modulus of elasticity of concrete) is less than that of normal concrete models for $f'c < 30\text{MPa}$ and greater than it for $f'c \geq 30\text{MPa}$.

REFERENCES

- [1] L.C. Bank, Ed., "*Composites for Construction: Structural Design with FRP Materials*", John Wiley & Sons, Inc., 2006.
- [2] ACI 440.2R-02, "*Guide for the Design and Construction of Externally Bonded FRP Systems for Strengthening Concrete Structures*", ACI Committee, American Concrete Institute, Farmington Hills, Michigan, USA, 2002.
- [3] D.J. Victor, N. Lakshmanan and N. Rajagoplan, "Ultimate Torque of Reinforced Concrete Beams", *Journal of Structural Division*, ASCE, vol. 102, no. ST7, pp. 1337-1352, 1976.
- [4] X.Z. Lu, J.G. Teng, L.P. Ye and J.J. Jiang, "Bond-Slip Models for FRP Sheets/Plates Bonded to Concrete", *Engineering Structures*, vol. 27, no. 6, pp. 920-937, 2005.
- [5] E.Y. Sayed-Ahmed, R. Bakay and N.G. Shrive, "Bond Strength of FRP Laminates to Concrete State-of-the-Art Review", *Electronic Journal of Structural Engineering*, vol. 9, pp. 45-61, 2009.
- [6] Y. Hiroyuki and Z. Wu, "Analysis of Debonding Fracture Properties of CFS Strengthened Member Subject to Tension", *Proceedings of 3rd international symposium (FRPRCS-3), non-metallic (FRP) reinforcement for concrete structures, Sapporo, Japan*, pp. 287–294, 1997.
- [7] T. Tanaka, "Shear Resisting Mechanism of Reinforced Concrete Beams with CFS as Shear Reinforcement", Graduation thesis, Hokkaido University, Japan, 1996.
- [8] T. Maeda, Y. Asano, T. Sato, T. Ueda and Y. Kakuta, "A Study on Bond Mechanism of Carbon Sheet", *Proceedings of 3rd international symposium (FRPRCS-3), nonmetallic (FRP) reinforcement for concrete structures*, vol. 1, pp. 279–286, Sapporo, Japan, 1997.
- [9] A. Khalifa, W.J. Gold, A. Nanni and A. Aziz, "Contribution of Externally Bonded FRP to Shear Capacity of RC Flexural Members", *ASCE Journal of Composites for Construction*, vol. 2, no. 4, pp. 195–203, 1996.

- Journal of University of Babylon for Engineering Sciences, Vol. (28), No. (1): 2020.
- [10] Y. Sato, T. Ueda, Y. Kakuta and T. Tanaka, "Shear Reinforcing Effect of Carbon Fibre Sheet Attached to Side of Reinforced Concrete Beams", *Proceedings of 2nd international conference on advanced composite materials in bridges and structures, Montreal: Canada*, pp. 621–627, 1996.
- [11] D.S. Yang, S.N. Hong and S.K. Park, "Experimental Observation on Bond Slip Behavior between Concrete and CFRP Plate", *International Journal of Concrete Structures and Materials*, vol. 1, no. 1, pp. 37–43, 2007.
- [12] J.F. Chen and J.G. Teng, "Anchorage Strength Models for FRP and Steel Plates Bonded to Concrete", *ASCE Journal of Structural Engineering*, vol. 127, no. 7, pp. 784–791, 2001.
- [13] B. Taljsten, "Plate Bonding: Strengthening of Existing Concrete Structures with Epoxy Bonded Plates of Steel or Fibre Reinforced Plastics", Ph. D. dissertation, University of Technology, Sweden, 1994.
- [14] H. Yuan and Z. Wu, "Interfacial Fracture Theory in Structures Strengthened with Composite of Continuous Fiber", *Proceedings of symposium of China and Japan: Science and technology of 21st century, Tokyo, Japan*, pp. 142–155, 1999.
- [15] T. Kanakubo, T. Furuta and H. Fukuyama, "Bond Strength between Fiber-Reinforced Polymer Laminates and Concrete", *Proceedings of 6th international RILEM symposium on non-metallic (FRP) reinforcement for concrete structures (FRPRCS-6), Singapore*, pp. 134–143, 2003.
- [16] J. Yao, J.G. Teng and J.F. Chen, "Experimental Study on FRP-to-Concrete Bonded Joints", *Composites Part B Engineering*, vol. 36, no. 2, pp. 99-113, 2005.
- [17] Y. Jain, "Debonding Failures in RC Beam and Slabs Strengthening with FRP Plates", Ph. D. dissertation, Department of Civil and Structural Engineering, Hong Kong Polytechnic University, 2004.
- [18] L. Zhao, "Characterizations of RC Beams Strengthened with Carbon Fiber Sheets", Graduation thesis, Department of Civil and Environmental Engineering, University of Alabama, Huntsville, Alabama, 2005.
- [19] ACI 318-14, "*Building Code Requirements for Reinforced Concrete*", ACI Committee, American Concrete Institute, Farmington Hills, Michigan, USA, 2014.
- [20] R.F. Gibson, Ed., "*Principles of Composite Material Mechanics*", McGraw-Hill, Inc., New York, 1994.
- [21] W.F. Chen, Ed., "*Plasticity on Reinforced Concrete*", McGraw-Hill Book Company, 1982.
- [22] P. Desayi and S. Krishnan, "Equation for the Stress-Strain Curve of Concrete", *Journal of the American Concrete Institute*, vol. 61, no. 3, pp. 345-350, 1964.

- Journal of University of Babylon for Engineering Sciences, Vol. (28), No. (1): 2020.
- [23] A. Kaw, Ed., "*Mechanical of Composite Materials*", CRC Press LLC, Boca Raton, Florida, USA, 1997.
- [24] Seracino (ed), "*FRP Composites in Civil Engineering – CICE 2004*", Taylor & Francis Group, London, pp. 556, 2004.
- [25] A. Carolin, "Carbon Fiber Reinforced Element for Strengthening of Structural Element", Ph. D. dissertation, University of Lulea Sweden, 2003.
- [26] ANSYS, "ANSYS Help", Release 15, 2014.

دراسة سلوكية رابطة الخرسانة-ألياف البوليمر للخرسانة الاعتيادية والخفيفة الوزن باستخدام طريقة العناصر المحددة

علي عدي هلال عهد زهير حمودي احمد صكبان سعدون
قسم الهندسة المدنية, كلية الهندسة, جامعة البصرة, البصرة, العراق.

ahmsag@gmail.com msc_eng_ah@yahoo.com ali.adi61@yahoo.com

الخلاصة

ان الهدف الرئيسي من هذه الدراسة هو دراسة سلوكية رابطة الخرسانة-الياف البوليمر لنوعين من الخرسانة (الخرسانة الاعتيادية والخرسانة الخفيفة الوزن) باستخدام خواص خرسانية مختلفة. وتم لهذا الغرض اختيار نموذج اختبار القص الاحادي ونمذجته باستخدام برنامج ANSYS. تم تمثيل النمذجة بطريقتين: بوجود مادة الايبوكسي اللاصقة (نموذج الايبوكسي) وبدون مادة الايبوكسي (نموذج الرابطة التامة). وتم تشكيل هذين النموذجين واستخدامهما في عملية التحليل. حُلَّت نماذج مختلفة من نوعين من الخرسانة (الاعتيادية والخفيفة الوزن) من أجل دراسة سلوك هذه الرابطة. لوحظ بأن نموذج الرابطة التامة أعطى نتائج أكثر توافقاً مع النتائج التجريبية المتاحة وأفضل من نموذج الايبوكسي. إذ إن معدل الفرق بين قوة الفشل التجريبية والتحليلية كان بمقدار 5.35% و 8.32% باستخدام نموذجي الرابطة التامة والايوكسي. على الترتيب. وقد وُجد أن الزيادة في مقاومة انضغاط الخرسانة تؤدي إلى زيادة في مقاومة الرابطة, حيث لوحظ أنه بزيادة مقاومة انضغاط الخرسانة من 20 الى 40MPa فإن مقاومة الرابطة لنماذج الخرسانة الاعتيادية والخفيفة الوزن قد ازدادت بحدود 81% و 106%, على الترتيب.

الكلمات الدالة: الياف البوليمر، رابطة، مقاومة الرابطة، اختبار القص الاحادي.